



Scope and limitation of activated carbons in aqueous organometallic catalysis

Nicolas Kania^{a,b,d}, Narasimhan Gokulakrishnan^{a,b,d}, Bastien Léger^{a,b,d}, Sophie Fourmentin^{a,c},
Eric Monflier^{a,b,d}, Anne Ponchel^{a,b,d,*}

^a Univ Lille Nord de France, F-59000 Lille, France

^b UArtois, UCCS, F-62300 Lens, France

^c ULCO, UCEIV, EA 4492, F-59140 Dunkerque, France

^d CNRS, UMR 8181, France

ARTICLE INFO

Article history:

Received 8 October 2010

Revised 6 December 2010

Accepted 7 December 2010

Available online 14 January 2011

Keywords:

Mass transfer

Activated carbons

Palladium

Phosphanes

TPPTS

Tsuji–Trost reaction

Biphasic catalysis

Sustainable chemistry

ABSTRACT

The effect of activated carbons has been studied in the palladium-catalyzed cleavage reaction of allylalkylcarbonate under aqueous biphasic conditions. A number of parameters were investigated, such as the type of carbon, the structure of the water-soluble ligand, the water conditions, and the metal complex loading. It was found that the intrinsic properties of carbons had a strong influence on the reaction rates. The best performances were obtained with the AC-WV carbon possessing the largest part of mesopores and lowest content of oxygen-surface groups. The results were rationalized by considering that AC-WV acted as a mass-transfer promoter increasing the interfacial area and collisions between the reactive species in the pore volume. The hypothesis of a confinement effect of the catalyst and reactants within the pores *via* adsorption–desorption processes was supported by isothermal studies and ³¹P{¹H} NMR investigations.

© 2010 Elsevier Inc. All rights reserved.

1. Introduction

Homogeneous catalysis plays a key role in carrying out chemical reactions in the most efficient way, thanks to the well-defined structure–property relationship between the molecular catalyst and the substrate. However, although the homogeneous catalysts are generally highly active and selective, these systems may suffer from difficulties associated with the separation of the catalyst from the reaction medium and their subsequent recycling.

These problems can be elegantly solved by using biphasic aqueous organometallic catalysis, in which the molecular metal complex is immobilized in the aqueous phase by water-soluble ligands. The catalyst can be easily recovered in active form at the end of reaction by decantation of the aqueous and organic phases, and the production costs are significantly lower [1,2]. One class of ligands, which attracts significant attention in aqueous organometallic catalysis, are phosphanes bearing sulfonated polar groups ($-\text{SO}_3^- \text{Na}^+$) to ensure a sufficient solubility in water. Notably, several industrial-scale plants based on aqueous biphasic technologies, using metal complexes stabilized by water-soluble phosphanes, are now operating. The most striking example is the Ruhrchemie/Rhône-Poulenc

process (now OXEA company), in which the rhodium associated with *meta*-trisulfonated triphenylphosphane (TPPTS; $\text{P}(m\text{-C}_6\text{H}_4\text{SO}_3\text{Na})_3$) catalyzes the hydroformylation of propene or butene [3]. Another industrial example concerns the hydrodimerization of butadiene and water by the Kuraray company. The process includes two catalytic steps in biphasic aqueous medium using palladium or rhodium, stabilized by *meta*-monosulfonated triphenylphosphane [TPPMS, $\text{PPh}_2(m\text{-C}_6\text{H}_4\text{SO}_3\text{Na})$] [3]. Although appropriate for water-soluble substrates, biphasic aqueous organometallic processes cannot be easily generalized, especially when considering the case of highly hydrophobic substrates for which mass-transfer limitations occur.

To circumvent the problems of solubility in water, a variety of strategies have been investigated, such as the utilization of co-solvents [4], amphiphilic phosphanes [5,6], polymers [7], surfactants [8–11], or cyclodextrins [12–16]. It is worth mentioning that some drawbacks can be associated with these methods. Indeed, surfactants and amphiphiles may give rise to foaming and persistent emulsions during the workup, whereas co-solvents or polymers can be difficult to remove from the products at the end of the reaction.

The possibility of performing organometallic-catalyzed reactions in aqueous media by using solid suspensions has also been viewed as an alternative method. The most striking example is that of supported aqueous-phase catalysis (SAPC) originally developed

* Corresponding author at: UArtois, UCCS, F-62300 Lens, France. Fax: +33 3 2179 1755.

E-mail address: anne.ponchel@univ-artois.fr (A. Ponchel).

by Davis et al. [17–20], whose principle is based on the use of a thin film of water to dissolve and disperse the water-soluble catalytic complex onto the surface of a hydrophilic porous support (mostly silica-based materials). This strategy has proven fruitful for the hydroformylation of olefins [21], selective hydrogenation of α,β -unsaturated aldehydes [22], asymmetric hydrogenation [23], and allylic alkylation [24]. The immobilized complex is assumed to work at the aqueous–organic interface in the water film, thus allowing a larger interfacial area. However, the main disadvantage of SAPC lies in the fact that the degree of hydration of the support must be carefully controlled in order to retain the catalyst on the solid surface without any metal leaching [21]. Recently, a slightly different approach was reported by Holmberg et al. [25] in the Heck-type reaction between an arylboronic acid and styrene by using an ordered mesoporous silica with a rhodium complex stabilized by *meta*-disulfonated triphenylphosphane [TPPDS; PPh(*m*-C₆H₄SO₃Na)₂]. The authors postulated that the reaction occurred at the interface between the organic and water domains, namely at the pore openings of the mesoporous silica and not at the surface of the particles.

The utilization of carbon materials in biphasic aqueous organo-metallic has not been the subject of extensive studies. This observation is surprising since aqueous suspensions of carbon particles are known to enhance gas–liquid [26–29] and liquid–liquid [30,31] mass transfers. Interestingly, carbon materials satisfy most of the desirable requirements to be used in catalytic processes, including a high porous volume, high surface area, thermal stability, and chemical inertness [32]. Furthermore, the fact that activated carbons can be produced from agricultural and forestry residues, or generally biomass residue wastes makes the applications even more appealing from the environmental point of view. In this context, the combined use of an activated carbon and a rhodium complex coordinated by water-soluble phosphane was initially reported by Luft et al. [33]. They explained the results obtained during the hydroformylation of 1-hexene by considering a supported aqueous-phase catalytic mechanism.

Recently, the possibility of using an activated carbon as a mass-transfer additive has been reported by our group [34]. Thus, we have described that the addition of a small amount of activated carbon could efficiently solve mass-transfer limitations in the Pd-TPPTS-catalyzed-Tsuji–Trost reaction with water-insoluble allylalkylcarbonates. It has been evidenced that the beneficial effect of the studied carbon was strikingly connected to the solubility of the substrates, i.e. the lower the solubility, the more important the contribution to the mass transfer. For instance, a reaction rate enhancement of 470 can be obtained with a very hydrophobic substrate, i.e. the allyloctadecylcarbonate [34]. In the present paper, we wish to examine in more details the effects of activated carbons on the activity of phosphane-coordinated palladium complexes in the cleavage of allylalkylcarbonates under biphasic conditions. A number of parameters will be investigated, such as the type of carbon, the oxidizing treatment, the structure of the water-soluble ligands, the water conditions, and the metal complex loading. The ability of activated carbons to promote the palladium-catalyzed-Tsuji–Trost reaction will be discussed on the basis of adsorption isotherm studies and ³¹P{¹H} NMR experiments. In conclusion, a rationale will be proposed to explain the promoting role of activated carbons during the course of the reaction.

2. Experimental

2.1. Chemicals

The sodium salt of *meta*-substituted trisulfonated triphenylphosphane (TPPTS) was synthesized according to a procedure

reported in the literature [35]. The synthesis of trisulfonated biphenylphosphanes, i.e. P(BiPh)₃TS, P(BiPh)₂PhTS, P(BiPh)Ph₂TS where Ph and BiPh correspond to phenyl and biphenyl groups, respectively, was performed by a procedure recently developed in our laboratory [36]. The ligand purities were carefully controlled by ¹H, ¹³C, and ³¹P{¹H} NMR analyses. In particular, ³¹P{¹H} NMR indicated that the products were mixture of phosphanes (ca. 98%) and oxides (ca. 2%). For NMR spectroscopy measurements, D₂O (99.92% isotopic purity) was purchased from Euriso-Top. All other reactants were purchased from Aldrich Chemicals and Acros Organics in their highest purity and used without further purification. Distilled deionized water was used in all experiments.

2.2. Carbons and their treatments

The starting activated carbons were selected from commercially available samples. The main part of the work was carried out using the Nuchar®WV-B-activated carbon (denoted AC-WV), which was a gift from MeadWestvaco Corporation (Covington, USA). It was produced from wood and activated by phosphorous acid. In some cases, Norit®SA-2 (denoted AC-NorA) and Sorbonorit®B3 (denoted AC-NorB), produced by Norit (Amersfoort, Netherlands) from peat and steam activated, were used for comparison.

To increase the number of acidic functions, the AC-WV carbon was treated with different concentrations of nitric acid, from 10⁻⁴ to 16 M. In a typical experiment, 1.0 g of carbon was stirred for 1 h with 100 mL of HNO₃ of a known concentration at room temperature or under reflux. After the treatment, the carbon was recovered by filtration, thoroughly washed with deionized water until the pH value of the washing water was the same as that of deionized water. The resulting carbon particles were dried in an oven at 100 °C overnight and finally ground to powder in an agate mortar. The solids are denoted AC-WVx where x corresponds to the initial concentration of nitric acid.

2.3. Characterization methods

The nitrogen adsorption/desorption isotherm was obtained at –196 °C by using a Nova 2200 apparatus from Quantachrome Corporation, after having degassed the sample overnight at 100 °C. The specific area was calculated from the Brunauer–Emmett–Teller (BET) equation using P/P_0 values between 2.5×10^{-3} and 1.7×10^{-1} , and the pore-size distribution was obtained from the desorption branch using the BJH method. The total pore volume was estimated at $P/P_0 = 0.95$, while the micropore volume was determined by the Dubinin–Radushkevich method. The average pore size was estimated from the ratio of the total pore volume to the BET surface area by the Gurvich's rule, assuming that the pores are of cylindrical geometry.

The Boehm's titration method was used to determine the number of acidic and basic groups [37]. In a typical experiment, 1.0 g of carbon sample was equilibrated for 24 h with 50 mL of NaHCO₃, Na₂CO₃, or NaOH solutions (0.05 mol L⁻¹). Then, 5 mL of each filtrate was titrated with HCl (0.05 mol L⁻¹). The numbers of acidic sites were calculated from the assumption that NaOH neutralizes carboxylic, phenolic, and lactonic groups, that Na₂CO₃ neutralizes carboxylic and lactonic, and that NaHCO₃ neutralizes only carboxylic groups. Basic surface sites were determined similarly by using HCl solution (0.05 mol L⁻¹) as reactant.

ATR-FTIR experiments were carried out in the 1800–900 cm⁻¹ region with a spectral resolution of 2 cm⁻¹ on a Shimadzu IR Prestige-21 spectrometer equipped with a MIRacleA Germanium prism.

The zeta potential (ζ) of the carbon materials was determined in water suspensions, using a Malvern Zetasizer Nano ZS (preparation: 1 mg of AC in 10 mL of deionized water). The ζ -potential

corresponds to the potential difference between the dispersion medium and the electrical double layer of fluid attached to the dispersed particle. The measurements are based on a Laser Doppler electrophoretic mobility of carbon particles *via* the Helmholtz–Smoluchowsky equation:

$$\zeta = (\eta/\varepsilon) \cdot \mu_e$$

where μ_e is defined as the ratio between the velocity of the carbon particles and the magnitude under the applied electric field, η is the viscosity of the suspending liquid and ε the dielectric conductivity of water.

The $^{31}\text{P}\{^1\text{H}\}$ NMR spectra were recorded on a Bruker Avance 300 DPX instrument at 75.46 MHz, respectively. The $^{31}\text{P}\{^1\text{H}\}$ chemical shift is given in ppm relative to the external reference that is H_3PO_4 in D_2O .

2.4. Catalytic procedure

The water-soluble phosphane (94.5 μmol , 9 equiv.) and $\text{Pd}(\text{OAc})_2$ (10.5 μmol) were dissolved in water (2.0 g) in a Schlenk tube and stirred with a magnetic bar for 4 h at room temperature under nitrogen atmosphere. The yellow solution was transferred by canula into another Schlenk tube containing the activated carbon (5 mg). The resulting catalytic suspension was stirred with a magnetic bar at room temperature for 17 h. Then, a mixture containing allylundecylcarbonate (0.64 mmol), diethylamine (1.28 mmol), and dodecane (0.32 mmol) used as internal standard was dissolved in heptane (1.2 g) and transferred into the catalytic suspension. The reaction was carried out at room temperature, and the stirring rate was adjusted accordingly (1250 rpm), so that external mass-transfer limitations were eliminated [34]. The reaction was monitored by analyzing aliquots of the reaction mixture (organic phase) with a Shimadzu GC-17A gas chromatograph, equipped with a methyl silicone capillary column (30 m \times 0.32 mm) and a flame ionization detector.

2.5. Interactions with the activated carbon

2.5.1. TPPTS adsorption isotherm

The ability of AC-WV to adsorb TPPTS was evaluated using the following procedure: in a round bottom flask and under nitrogen atmosphere, AC-WV (25 mg) was suspended in 5 mL of TPPTS of a known concentration and vigorously stirred for 4 h at room temperature. After elimination of the solid phase by filtration, the absorbance of the solution was analyzed at 250 nm by a UV–Vis Lambda 19 Perkin-Elmer spectrophotometer. The experimental data for the uptake of TPPTS were treated according to the Langmuir and Freundlich equations. The Langmuir model is based on a monolayer adsorption with a uniform energy of adsorption and characterized by the following equation:

$$q_e = \frac{K_L \cdot q_0 \cdot C_e}{1 + K_L \cdot C_e}$$

where q_e is the equilibrium amount of solute per unit mass of activated carbon (mg g^{-1}), q_0 is the maximum adsorption per unit mass of activated carbon (mg g^{-1}), C_e is the equilibrium concentration (mg L^{-1}), and K_L is the Langmuir equilibrium constant.

In contrast to the theory of Langmuir, the Freundlich equation is derived from an empirical model, in which the energy of adsorption varies exponentially with surface coverage, according to the following equation:

$$q_e = K_F \cdot (C_e)^{1/n}$$

where q_e is the equilibrium amount of solute per unit mass of activated carbon (mg g^{-1}), C_e is the equilibrium concentration (mg L^{-1}),

K_F is the Freundlich equilibrium constant, and $1/n$ is an empirical dimensionless constant related to the magnitude of the adsorption driving force.

2.5.2. $^{31}\text{P}\{^1\text{H}\}$ NMR study of the $\text{Pd}(\text{TPPTS})_3$ complex

$\text{Pd}(\text{TPPTS})_3$ in a D_2O solution was synthesized according to a modified literature procedure [38]. In a Schlenk tube, $\text{Pd}(\text{PPh}_3)_4$ (103 mg, 0.09 mmol) was dissolved in 2 g of previously degassed toluene under nitrogen atmosphere. TPPTS (76 mg, 0.13 mmol) was dissolved in 2 g of previously degassed D_2O and then transferred by canula to the organic palladium solution. The biphasic medium was stirred for 0.5 h at room temperature. After decantation, the aqueous phase was recovered. This solution contained the expected palladium catalyst $\text{Pd}(\text{TPPTS})_3$ and an excess of about 10% of free TPPTS (with regard to the initial amount of TPPTS). Studies in the presence of activated carbon were conducted as follows: to the required amount of AC-WV was introduced 500 μL of the above $\text{Pd}(\text{TPPTS})_3$ solution under nitrogen atmosphere. After 4 h of stirring, the resulting solution was transferred by canula into a nitrogen pressurized 5 mm NMR tube and the $^{31}\text{P}\{^1\text{H}\}$ NMR spectrum was recorded.

3. Results

3.1. Carbon characterizations

Before examining the behavior of carbons in aqueous organometallic catalysis, physicochemical characterizations have been undertaken. Thus, the nitrogen sorption isotherms of the unmodified commercial carbons are reported in Fig. 1, whereas the corresponding textural parameters are gathered in Table 1.

Among the three starting carbons, the MeadWestvaco AC-WV carbon is the one which develops the highest surface area (1690 $\text{m}^2 \text{g}^{-1}$) and largest pore size (3.1 nm). It exhibits a composite type I–II isotherm, consistent with a combined micro- and mesoporosity, as shown on the BJH pore-size distribution with sizes in the 2–10 nm range. In comparison, the plateaux in the N_2 uptakes observed for AC-NorA and AC-NorB suggest that the materials are essentially microporous, with 60% and 75% of the total pore volume occupied by micropores, respectively. Concerning the pore size, it can be noted that the higher the microporosity percentage,

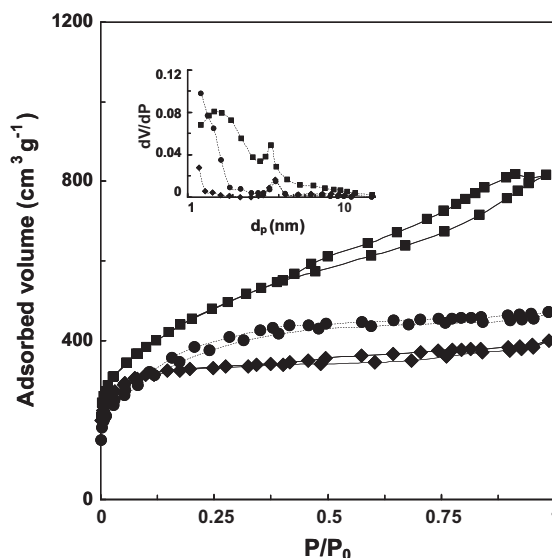


Fig. 1. Nitrogen adsorption isotherm and BJH pore-size distribution of AC-WV (■), AC-NorA (●), and AC-NorB (◆) carbons.

Table 1

Textural characteristics of the starting carbon supports.

Carbon	S_{BET} ($\text{m}^2 \text{g}^{-1}$)	V_{tot} ($\text{cm}^3 \text{g}^{-1}$)	V_{micro} ($\text{cm}^3 \text{g}^{-1}$)	% Micro ^a	Average pore diameter (nm)
AC-WV	1690	1.32	0.54	41	3.1
AC-NorA	1207	0.71	0.42	60	2.4
AC-NorB	1224	0.60	0.45	75	2.0

^a Relative percentage of microporosity defined as the ratio of the micropore volume to the total pore volume.

the smaller the average pore size. Although the pore size calculation based on the Gurvich's rule is not the most accurate method, it gives nevertheless an idea of the differences in pore size in the materials. Thus, the pore size of AC-NorB is in the range of micropores (2.0 nm), whereas for AC-NorA and AC-WV, the average pore sizes are in the mesopore range (2.4 and 3.1 nm, respectively).

Another important concern is the determination of the surface compositions by the Boehm's titrations. As shown by results reported in Table 2, the AC-WV carbon presents a variety of species mainly acid, likely due to its origin and method of activation with phosphoric acid. However, the total amount of sites remains low, i.e. $39 \mu\text{mol g}^{-1}$ corresponding to a surface density of 0.02 function per nm^2 (entry 1 in Table 2). This result is consistent with a carbon surface almost free from oxygen functional groups. Note that this assumption has been further supported by EDX analysis showing that AC-WV mostly contains the carbon element in its matrix (Fig. S1 in the Supplementary material). Thus, the presence of silicon, aluminum, and phosphorus is detected in trace amount. These elements could be the result of the synthesis process of the activated carbon, like phosphorus coming from the activation step by phosphoric acid. This analysis also corroborates with the XPS surface analysis, whose spectrum indicates a surface composition of 94.6% carbon and 5.6% oxygen (Fig. S2 and Table S1 in the Supplementary material). Thus, the resulting O/C surface ratio, i.e. 0.59, is in agreement with the total acidity measured by Boehm's titration on the basis of the relationship established by Devillers et al. [39]. In contrast, it is shown that AC-NorA and AC-NorB possess more functionalized surfaces. Indeed, the total number of surface sites (acid and basic) is 14 and 7 times higher, respectively, than that measured with the unmodified AC-WV sample (entries 2–3 in Table 2). More precisely, the titrations indicate that AC-NorB is the most acidic support with $201 \mu\text{mol g}^{-1}$ of total acid functions, whereas AC-NorA develops the highest basic character. In line with what is usually observed, the oxidation of AC-WV by nitric acid leads to an increasing number of oxygen containing groups, in almost each category; the stronger the treatment, the higher the number of acidic functions. For instance, the most highly functionalized material (HNO_3 16 M for 1 h under reflux) displays a total acidity of $1421 \mu\text{mol g}^{-1}$ corresponding to 1.1 functions per nm^2 (entry 8 in Table 2).

Further spectroscopic evidence of the presence of oxygen containing organic functional groups after oxidative treatments has been obtained using FTIR spectroscopy (Fig. 2). The spectrum of the unmodified AC-WV shows weak bands at ca. 1570, 1200, and 1020 cm^{-1} ascribed to the vibrational modes of the carbon matrix [$\nu(\text{C}=\text{O})$, $\nu(\text{C}=\text{C})$ or $\nu(\text{C}-\text{O})$, and $\nu(\text{O}-\text{C}-\text{O})$, respectively]. With acid treatments, these bands are magnified. An additional band at 1750 cm^{-1} is also revealed, which indicates the formation of carboxylic and lactonic groups on the edges of layers planes. According to the literature [40], the carbon atoms located at the periphery of the layer (so-called edge sites) exhibit higher reactivity toward oxidation than those within the basal plane sites and surrounded by other carbon atoms. Concurrently to the changes in the nature and concentration of the surface functionalities, it is also shown in Table 2 that the specific areas are affected by the oxidation treatment of AC-WV with nitric acid. This tendency may reflect the alteration of the carbon matrix by introduction of oxygen groups

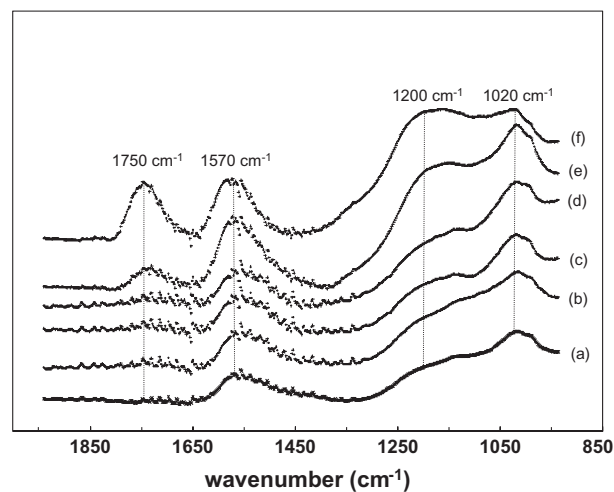


Fig. 2. Effect of the nitric acid treatments on the ATR-FTIR spectra of AC-WV: (a) untreated support and treated with different concentrations of nitric acid, (b) 0.0001; (c) 0.001; (d) 0.01; (e) 0.1; and (f) 16 mol L^{-1} .

Table 2

Characteristics of the starting and modified carbons in terms of specific areas, Zeta potentials and Boehm's titrations.

Entry	Carbon	Treatment	Temperature conditions	C_{HNO_3} (mol L^{-1})	S_{BET} ($\text{m}^2 \text{g}^{-1}$)	ζ (mV) ^a	Titration results ($\mu\text{mol g}^{-1}$)					
							Carboxylic	Lactonic	Phenolic	Acidic	Basic	Total
1	AC-WV	No	–	–	1690	–30.0	4	11	19	34	5	39
2	AC-NorA	No	–	–	1207	–34.1	1	8	37	46	493	539
3	AC-NorB	No	–	–	1224	–42.7	77	1	123	201	71	272
4	AC-WV.0001	Yes	r.t. ^b	10^{-4}	1540	–31.4	5	13	35	53	–	53
5	AC-WV0.001	Yes	r.t. ^b	10^{-3}	1380	–32.8	10	10	70	90	–	90
6	AC-WV0.01	Yes	r.t. ^b	10^{-2}	1286	n.d. ^c	50	20	151	221	–	221
7	AC-WV0.1	Yes	Reflux	10^{-1}	917	–34.7	85	126	120	332	–	332
8	AC-WV16	Yes	Reflux	16	776	–48.9	407	484	530	1421	–	1421

^a Zeta-potential measurements performed in water. The standard deviations, calculated by means of three replicates, were within ± 2 mV.^b Room temperature.^c Non-determined value.

and removal of some carbon atoms [41]. The formation of surface oxygen groups at the entrance to the pores may also obstruct N_2 access to the micropores [42].

However, it should be also noted that the carbon structure was not completely denatured after acid treatment. With this objective, electron microscopy investigations have been performed on AC-WV and AC-WV16 (Fig. S3 in the Supplementary material). Thus, we observe from the Scanning Electron Microscopy (SEM) images taken at the same magnification that the acid treatment provides a notable decrease in the carbon particle size. Note that this last effect has also been confirmed by laser granulometry measurements, which indicate medium particle sizes (d_{50}) of 36 and 7 μm for AC-WV and AC-WV16, respectively (Fig. S4 in the Supplementary material). The effect of the oxidation treatment is also revealed in the EDX spectrum with the appearance of an intense band $K_{\alpha 1}$ at ca. 0.5 keV characteristic of the oxygen element (Fig. S5 in the Supplementary material). A more detailed examination of the structure of carbons is obtained at a higher magnification by Transmission Electron Microscopy (TEM). In both cases, the TEM images exhibit a similar internal structure made of a disordered entanglement between carbon sheets.

To evaluate the impact of the degree of the surface functionalization on the stability of the carbon suspensions, zeta-potential measurements have been carried out in water (Table 2). Indeed, this technique is considered to be a useful indicator to evaluate the balance between the repulsive and attractive forces in solid suspensions. Thus, it is generally assumed that carbon particles, with zeta potentials more positive than +30 mV or more negative than -30 mV, form stable suspensions in water. Regarding the unfunctionalized AC-WV, the zeta potential (in absolute value) is rather lower than those obtained with AC-NorA and AC-NorB (30 vs 34.1 and 42.7 mV, respectively). This result can be related to the fact that AC-WV possesses the lowest content of oxygen-surface groups. This assumption concurs with the results obtained after acid treatment, for which the zeta-potential values become higher with the gradual increase in the number of oxygen acidic groups in the backbone of the carbon structure. This effect can be rationalized by an increase in the surface densities of charged functional groups, giving rise to enhanced electrostatic repulsions and enhanced stabilities of the carbon suspensions in water.

3.2. Aqueous organometallic catalysis

3.2.1. Cleavage of allylundecylcarbonate

The carbon materials have been tested in the cleavage reaction of allylundecylcarbonate under biphasic aqueous conditions and in the presence of diethylamine as the allyl scavenger (Scheme 1). The catalytic species are formed by in situ reduction of $\text{Pd}(\text{OAc})_2$ with 9 equiv. of phosphane. This procedure has the great advantage to avoid the tedious steps of synthesis and purification of the $\text{Pd}(\text{TPPTS})_3$ complex [38].

When comparing the allylundecylcarbonate conversion over time, it is readily apparent that the reaction occurs very slowly when the experiment is conducted without any addition of activated carbon (Fig. 3). This result confirms that the limiting step of the reaction is the mass transfer. Whereas the addition of AC-NorB is inadequate to improve the reaction rate, we observe that AC-NorA and AC-WV, especially, appear to be valuable mass-transfer agents in the Tsuji–Trost reaction since much higher levels of

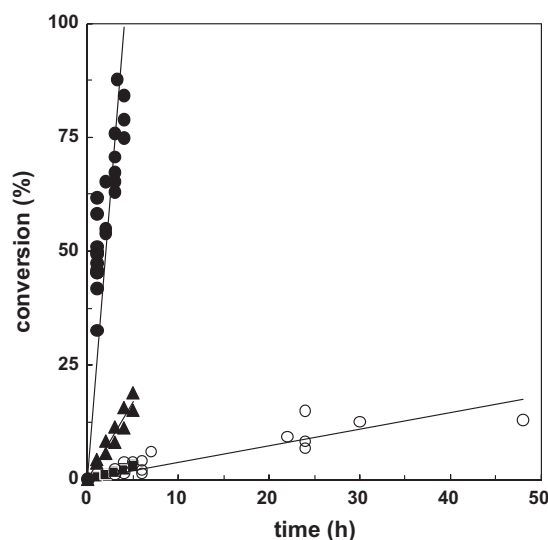


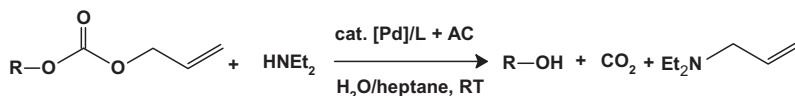
Fig. 3. Conversion of allylundecylcarbonate in the $\text{Pd}(\text{TPPTS})_3$ -catalyzed cleavage reaction as a function of time without (\circ) and with activated carbon in the reaction medium: AC-NorB (\blacksquare), AC-NorA (\blacktriangle), and AC-WV (\bullet).

conversion are obtained. Thus, the conversions reach 13% and 79% after 4 h reaction in the presence of AC-NorA and AC-WV, respectively, vs 2.3% in the presence of AC-NorB (entries 2–4 in Table 3). Note that AC-WV is by far the most efficient promoter, with a relative reaction rate (ratio of the initial activity with AC to that measured without AC) achieving a factor of 83 by using 5 mg of additive. This result suggests that the addition of carbon particles leads to higher mass transfer as a result of higher interfacial area between the aqueous and organic phases. Interestingly, a twofold increase in the AC-WV loading results in a twofold increase in the reaction rate (entry 5 in Table 3), whereas further addition of carbon decreases the catalytic efficiency per unit surface (entries 6–8 in Table 3).

Two factors can account for the higher efficiency of AC-WV.

The first one is the pore-size distribution, which has to be adequate to adsorb the allylundecylcarbonate substrate with a minimum of steric hindrance [43]. Among the materials studied here, it has already been reported that AC-WV possessed the broadest pore-size distribution, with most of the pores in the 2–10 nm range. Thus, for a similar range of amount of surface acid sites and specific surface area ($200 \mu\text{mol}^{-1}$ and $1200\text{--}1300 \text{m}^2 \text{g}^{-1}$, respectively), our results suggest that carbons having the highest proportion of mesopores remain the best carriers to promote the Tsuji–Trost reaction (21.0 vs 3.5mol h^{-1} for the AC-WV0.01 and AC-NorB, respectively). These textural features should facilitate the adsorption and diffusion of the long-alkyl chain allylcarbonate, from the organic phase to the aqueous phase that contains the catalyst.

The second one is the quasi absence of oxygenated function at the surface of the material. Indeed, experiments conducted in the presence of the oxidized AC-WV samples with varying degree of functionalization show that the overall reaction rate is drastically reduced with increasing content of oxygenated groups (Fig. 4). We assume that the incorporation of oxygen acidic groups makes the surface more polar, thereby leading to a decrease in the



Scheme 1. Palladium-catalyzed cleavage of allylalkylcarbonate (Tsuji–Trost reaction).

Table 3
Cleavage of the allylundecylcarbonate over Pd(TPPTS)₃ using activated carbons.^a

Entry	Additive	Weight (mg)	Initial reaction rate ^b ($\mu\text{mol h}^{-1}$)	Relative reaction rate ^c	Initial areal rate ^d ($\mu\text{mol h}^{-1} \mu\text{mol}_{(\text{Pd})}^{-1} \text{m}^{-2}$)	Conv. ^e (%)
1	–	–	3.7	–	–	2.5
2	AC-NorB	5	3.5	0.9	0.05	2.3
3	AC-NorA	5	25.2	6.8	0.40	13
4	AC-WV	5	307	83	3.7	79
5	AC-WV	10	640	174	3.9	100
6	AC-WV	20	956	258	2.9	100
7	AC-WV	40	1176	318	1.8	100
8	AC-WV	70	1281	346	1.1	100
9	AC-WV.0001	5	262	71	3.2	56 ^f
10	AC-WV0.001	5	210	57	2.9	50 ^f
11	AC-WV0.01	5	21.0	5.7	0.3	10.5
12	AC-WV0.1	5	5.3	1.4	0.1	3.3
13	AC-WV16	5	0	–	0	0 ^g
14 ^h	AC-WV16	5	493	–	–	100 ^h

^a Reaction conditions: Pd, 10.5 μmol ; TPPTS, 94.5 μmol ; Water, 2.0 g; Allylundecylcarbonate, 0.64 mmol; Diethylamine, 1.28 mmol, C₁₂H₂₆ (internal standard), 0.32 mmol; Heptane, 1.2 g; Room temperature; Stirring rate, 1250 rpm.

^b Defined as the number of micromoles of allylundecylcarbonate converted per hour and calculated from the conversion measured at 30 min.

^c Defined as the ratio of the initial reaction rate in the presence of AC to that without AC.

^d Defined as the number of micromoles of allylundecylcarbonate converted per hour per micromoles of palladium and per surface area (on the basis of the specific surface area) and calculated from the conversion measured at 30 min.

^e After 4 h of reaction.

^f After 2 h of reaction.

^g After 7 h of reaction.

^h Addition of α -randomly methylated cyclodextrin (100 mg) in the reaction mixture of the run 13 after the 7 h of test. α -CDs are water-soluble cyclic oligosaccharides formed of 6 glucopyranose units exhibiting a hydrophobic cavity that can form inclusion complexes with of a wide variety of organic molecules. This property can be exploited in aqueous biphasic catalysis to solve mass-transfer limitations [12].

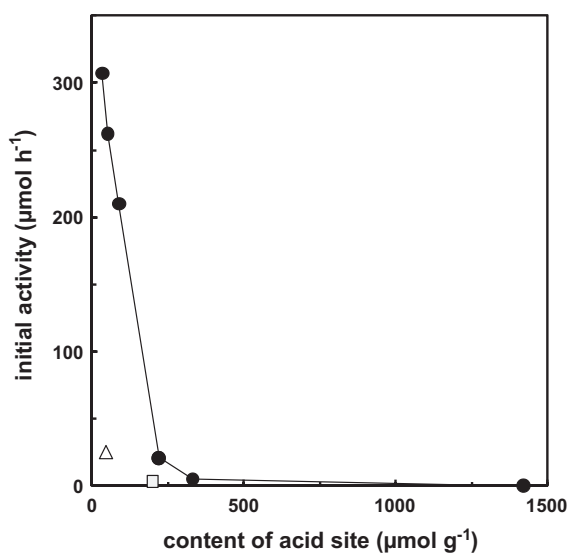


Fig. 4. Effect of the surface functionalization on the initial rate of allylundecylcarbonate cleavage over Pd(TPPTS)₃ with (Δ) AC-NorA, (\square) AC-NorB, and (\bullet) AC-WV series treated by nitric acid.

mass-transfer capacity toward the highly hydrophobic substrate, i.e. the allylundecylcarbonate. This interpretation is in line with studies in the literature dealing with the relationship between surface chemistry of activated carbons and adsorption of organic pollutants [44,45]. Note that the oxidative treatments do not provide any irreversible degradation of the catalytic complex. Indeed, whereas no catalytic activity is measured in the presence of AC-WV16 after 7 h of reaction (entry 13 in Table 3), the catalytic activity can be recovered by adding a typical water-soluble mass-transfer agent, i.e. the methylated- α -cyclodextrin (RaMe- α -CD) [12], in the reaction medium. Thus, immediately after the addition of RaMe- α -CD at the end of the 7-h test of Run 13, we observe a

rapid increase in the conversion, reaching 100% in 2 h (entry 14 in Table 3). This last result proves that the inhibition of the reaction observed in the presence of AC-WV16 alone is due to the alteration of the mass-transfer capacity of this functionalized carbon.

3.2.2. Influence of the water content

The effect of water content has been also examined (Fig. 5). It is found that, by using AC-WV, the initial activities remain low over a wide range of water contents, i.e. until 85 wt.% and that no maximum is observed for water contents close to the pore filling (10 wt.% of water). Thus, our results show that only large amounts of water can ensure proper conditions for catalysis, and this behavior is strongly different from what is usually described in SAPC. Indeed, it is usually assumed that the highest activities are achieved

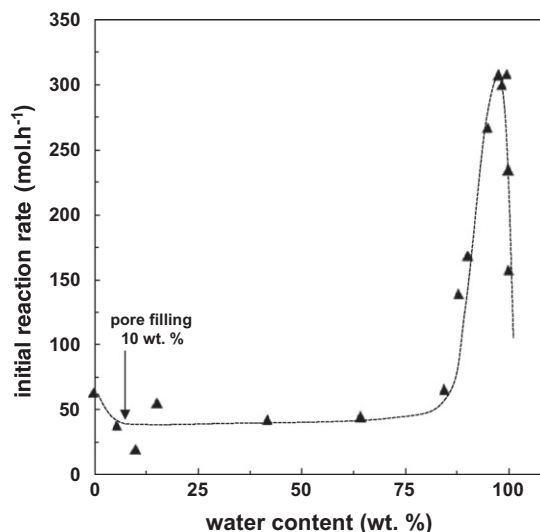


Fig. 5. Effect of the amount of water on the initial reaction rate in the Pd (TPPTS)₃-catalyzed cleavage reaction of allylundecylcarbonate.

with a low degree of pore filling and that slight deviations from the optimum of water content inevitably lead to reduced activities [21].

In our case, optimal conditions require large amounts of water to counterbalance the preferential adsorption of the organic substrate. Thus, it is proposed that, at these high water loadings, the carbon allows the mass transfer of the organic substrate by adsorption and the mixing with the aqueous phase containing the water-soluble metallic complex, leading to more effective interfacial areas.

3.2.3. Influence of the palladium loading

In order to gain deeper insight into the understanding of the catalytic process assisted by AC-WV, the influence of the complex loading, i.e. Pd(OAc)₂ and TPPTS, has been further examined. It should be emphasized that the total content of diethylamine remains here constant.

As shown in Fig. 6, two different domains are observed. Above 5 μmol of palladium (zone I), the cleavage reaction rates are independent of the palladium concentration, with a value close to 310 μmol h⁻¹. The resulting linear relationship confirms that the overall rate of the Tsuji–Trost reaction is limited by the diffusion of the allylundecylcarbonate at the interfaces and not by the kinetics of the reactions of the catalytic cycle. Below 5 μmol (zone II), we observe that the activity rises sharply with decreasing palladium loading. This effect is caused by the leaching of palladium from the aqueous to organic phase, associated with a ligand exchange reaction occurring between the coordinated-TPPTS and the nucleophilic diethylamine (Scheme 2). Thus, the equilibrium displacement becomes prominent when the HNEt₂/TPPTS ratio is very high (above ca. 30). Similar observations have already been reported in palladium-catalyzed Heck reactions [46].

3.2.4. Use of other water-soluble phenylphosphane ligands

The nature of the ligand is known to have a large influence on the overall rates of catalytic reactions carried out under aqueous biphasic conditions. This is usually attributed to a combination of

electronic, steric, or interfacial factors. To determine whether all water-soluble phosphane exhibit activity enhancements in the presence of the carbon additive, the behavior of different palladium/water-soluble phosphane combinations has been studied in the cleavage reaction of allylundecylcarbonate. In order to ensure high water solubility, the ligands are based on the backbone of TPPTS, with the substitution of one or more 3-sulfonatophenyl groups by 4-sulfonatobiphenyl groups. The results are reported in Table 4.

The promoting effect of AC-WV in the cleavage reaction is influenced by the chemical structure of the ligand itself. Thus, the relative reaction rates, measured in the presence or absence of carbon, for P(BiPh)₃TS, P(BiPh)₂PhTS, and P(BiPh)Ph₂TS are ca. 75, 4, and 1.7 times lower than that measured by using TPPTS. The efficiency of AC-WV seems to depend on the number of sulfonatobiphenyl groups in the phosphane unit; thus, the higher the sulfonatobiphenyl group content, the less important the beneficial contribution of AC-WV. These observations can be related to an alteration of the mass-transfer properties of the carbon, when the metal complex is stabilized by phosphanes of higher molecular weights.

4. Discussion

Starting from the previous results, we think that the palladium catalytic system, in the presence of activated carbons, could be controlled by different adsorption–desorption processes. On this basis, it can be hypothesized that, in addition to the adsorption of the organic substrate, the palladium complex coordinated by sulfonated phosphanes could also interact with the carbon surface. Remembering that Pd(TPPTS)₃ in the presence of AC-WV remains the best combination to promote the cleavage reaction, we have focused the investigations on this particular system.

Evidence for the affinity of TPPTS toward the carbon surface has been demonstrated from isothermal adsorption measurements performed in aqueous solutions at room temperature. The experimental sorption capacity is shown in Fig. 7, and the parameters of

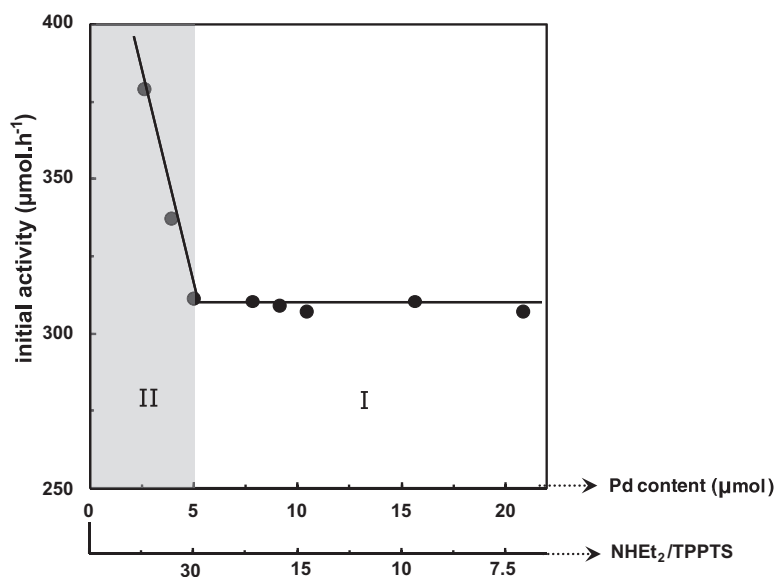
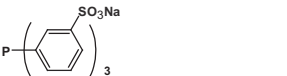
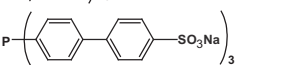
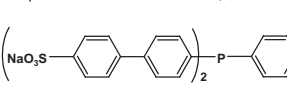
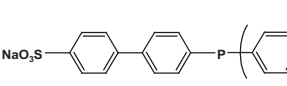


Fig. 6. Effect of the palladium content and diethylamine/phosphane ratio on the initial reaction rate of the cleavage of allylundecylcarbonate over Pd(TPPTS)₃ in the presence of AC-WV.



Scheme 2. Ligand exchange between the TPPTS-coordinated palladium and diethylamine.

Table 4
Catalytic performance of PdL₃ systems stabilized by different water-soluble phosphanes in the presence or absence of AC-WV.

Ligand	Structure	Reaction rate without AC ^a ($\mu\text{mol h}^{-1}$)	Reaction rate with AC ^b ($\mu\text{mol h}^{-1}$)	Conv. ^c (%)	Relative reaction rate ^d
TPPTS		3.7	307	48	83
P(BiPh) ₃ TS		2.3	2.5	0.4	1.1
P(BiPh) ₂ PhTS		14	288	45	21
P(BiPh)Ph ₂ TS		<1	44	6.9	~50

^a Reaction conditions: AC-WV, 5.0 mg; Pd, 10.5 μmol ; Ligand, 94.5 μmol ; Water, 2.0 g; Allylundecylcarbonate, 0.64 mmol; Diethylamine, 1.28 mmol, C₁₂H₂₆ (internal standard), 0.32 mmol; Heptane, 1.2 g; Room temperature; Stirring rate 1250 rpm.

^b Defined as the number of micromoles of allylundecylcarbonate converted per hour and calculated from the conversion measured at 30 min.

^c Conversion (%) in the presence of AC-WV after 1 h.

^d Defined as the ratio of the initial reaction rate in the presence of AC to that without AC.

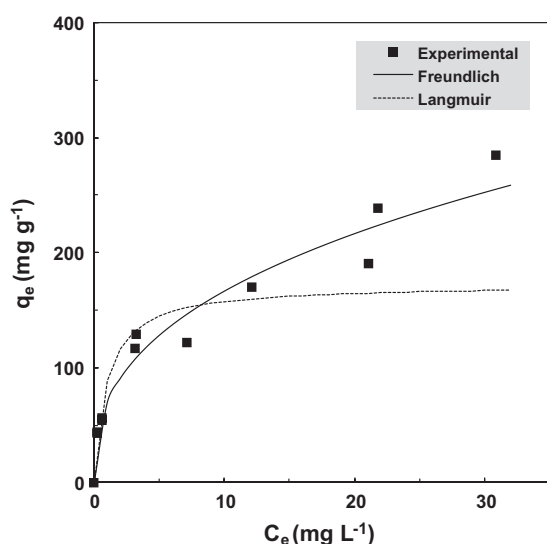


Fig. 7. Adsorption isotherms of TPPTS onto AC-WV: (■) experimental uptake and model adsorption isotherms obtained from the Freundlich (solid line) and Langmuir (dotted line) parameters.

the Langmuir and Freundlich models are given in Table 5. Based on the correlation coefficients of the linear regressions, the uptake data seem to be best described by the Freundlich equation. Thus, the modeling curve (solid line) constructed from the K_F and $1/n$ values fits the experimental data in a very satisfactory way. A resulting $1/n$ value of 0.379 is found, suggesting that the adsorption of TPPTS takes place easily on AC-WV. Indeed, it has already been proposed that the Freundlich isotherms could be classified in five common types of curves depending on the $1/n$ value and that a value between 0.1 and 0.5 was indicative of favorable adsorption conditions [47].

Furthermore, the ability of the Pd(TPPTS)₃ metallic complex to be adsorbed onto AC-WV has also been proved by ³¹P{¹H} NMR spectroscopic studies, performed in D₂O under nitrogen atmosphere (Fig. 8 and Table 6). Pd(TPPTS)₃ was synthesized using a procedure described by Hermann et al. that involves ligand exchange reactions between Pd(PPh₃)₄ and TPPTS [38].

Without addition of AC-WV, the spectrum reveals two main signals (Fig. 8a). The broad peak at $\delta_1 = 20.459$ ppm is ascribed to the Pd(TPPTS)₃ complex in equilibrium with ca. 10% of free TPPTS,

Table 5
Langmuir^a and Freundlich^b parameters calculated from the adsorption of TPPTS on AC-WV.

	Isotherm equation	Parameters	r^2
Langmuir	$q_e = \frac{180.6 C_e}{1 + 1.047 C_e}$	$q_0 = 172.4 \text{ mg g}^{-1}$, $K_L = 1.047 \text{ L mg}^{-1}$	0.9386
Freundlich	$q_e = 69.4 \cdot (C_e)^{0.379}$	$1/n = 0.379$, $K_F = 69.4$ ($\text{mg g}^{-1})(\text{L mg}^{-1})^{1/n}$)	0.9753

^a Langmuir linearization: $\frac{1}{q_e} = \frac{1}{q_0} + \frac{1}{q_0 K_L} \cdot \frac{1}{C_e}$.

^b Freundlich linearization: $\log q_e = \log K_F + (1/n) \cdot \log C_e$.

whereas the peak at $\delta_2 = 34.598$ ppm is attributed to trace amounts of TPPTS oxide. In agreement with previously reported data in the literature, the δ_1 chemical shift corresponds to an average value resulting from fast exchanges, occurring between the TPPTS-coordinated Pd and the free TPPTS [48–50]. By adding 5 mg of AC-WV into the Pd(TPPTS)₃ solution, the spectrum reveals a narrowing and a low-field shift of the δ_1 signal, concurrently to the decrease in the peak area (Fig. 8b). These effects are still more visible with 10 mg of AC-WV (Fig. 8c). These changes observed in the NMR spectra suggest that the addition of AC-WV causes an equilibrium displacement between the coordinated and un-coordinated TPPTS species, associated with a slower exchange rate. This phenomenon could only be explained by assuming the spontaneous adsorption of the free TPPTS and palladium complex *via* the TPPTS ligand on the support.

In line with the interpretation of Kalck et al. [48], the progressive shift of the δ_1 signal toward lower fields indicates the progressive increase in the ratio of TPPTS-coordinated Pd(0) to that of free TPPTS. We explain this behavior by the increasing removal of TPPTS from the aqueous solution due to the adsorption on the carbon surface. Thus, for the highest AC-WV loading, we have estimated that ca. 42% of the initial amount of phosphane (i.e. free or coordinated) was adsorbed onto the carbon support, corresponding to a coverage capacity of 800 mg g^{-1} (Table 6).

To complete this study, a last NMR investigation has been performed in order to study the evolution of the adsorption phenomenon under conditions close to those encountered during the aqueous biphasic catalytic process. Thus, competitive ³¹P{¹H} NMR titrations of TPPTS in D₂O have been carried out in the presence of allylundecylcarbonate as the competitor. Experiments are performed in the following manner: 10 mg of TPPTS and 10 mg of AC-WV (both in 1 mL of D₂O) are added to a defined volume of

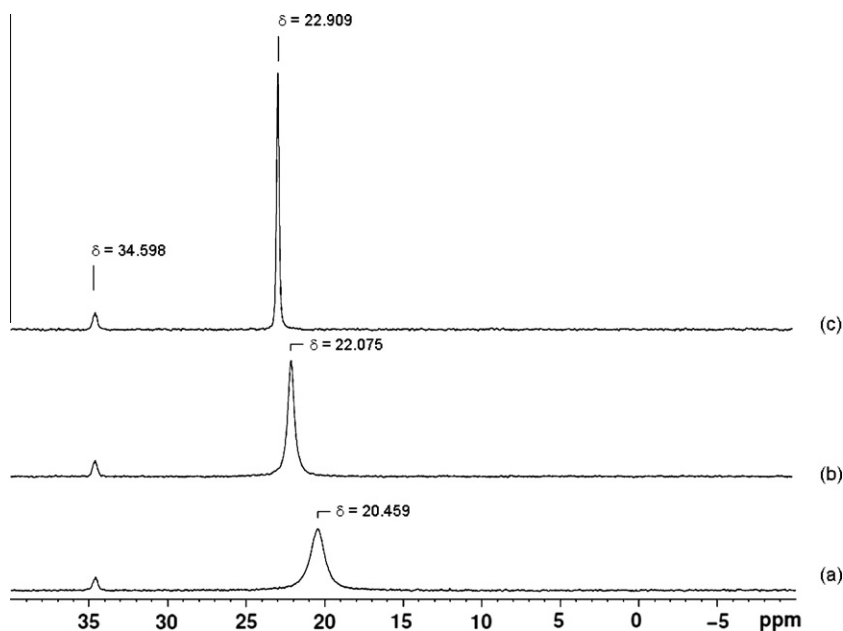


Fig. 8. Effect of the AC-WV support on the $^{31}\text{P}\{^1\text{H}\}$ NMR spectrum of $\text{Pd}(\text{TPPTS})_3$ in D_2O at 25 °C: (a) without activated carbon, (b) in the presence of 5 mg of AC-WV, and (c) in the presence of 10 mg of AC-WV.

Table 6

$^{31}\text{P}\{^1\text{H}\}$ NMR characteristics of $\text{Pd}(\text{TPPTS})_3$ adsorption onto AC-WV.^a

AC-WV (mg)	Free TPPTS (%)	TPPTS-coordinated Pd(0) (%)	Adsorbed TPPTS (%)	Adsorbed TPPTS (mg g^{-1})
0	10	90	0	0
5	3	79	18	720
10	~0	58	42	800

^a The relative amount of each type of TPPTS phosphane, i.e. free and coordinated-Pd(0), is deduced from the integrated peak intensity and the chemical shift of the δ_1 peak in the $^{31}\text{P}\{^1\text{H}\}$ NMR spectra. The amount of free TPPTS is calculated by assuming that the chemical shift is the weighted average of the characteristic peaks of $\text{Pd}(\text{TPPTS})_3$ and free TPPTS at δ 23.0 and -5.6 ppm, respectively.

organic phase (allylundecylcarbonate dissolved in heptane). The mixture is shaken for 4 h at room temperature under nitrogen atmosphere, and the solution was transferred *via* canula into the NMR tube prior to the acquisition of the spectrum (Fig. 9).

In comparison with the reference spectrum of TPPTS in D_2O (Fig. 9a), it is readily apparent that the presence of AC-WV causes a significant decrease in the relative intensity of the free TPPTS signal ($\delta_3 = -6.3$ ppm) due to its adsorption on the support (Fig. 9b). In these conditions, the percentage of adsorbed TPPTS is estimated to be ca. 40%.¹ Addition of allylundecylcarbonate to the aqueous suspension AC-WV and TPPTS gives rise to an intensity increase in δ_3 , showing that the affinity of TPPTS for the carbon surface is affected by a small amount of the hydrophobic competitor (Fig. 9c). Thus, the percentage of adsorbed TPPTS is reduced from 40% to 28%. Note that this last value remains almost constant with further increments of allylundecylcarbonate (Fig. 9d and e). These results can be explained by a partial exchange reaction occurring between the surface-adsorbed TPPTS and allylundecylcarbonate of the organic phase. We assume that this phenomenon is connected to different adsorption equilibrium constants. Interestingly, it should be also emphasized that the removal of TPPTS from the surface by allylundecylcarbonate is not complete, since the intensity of the original signal δ_3 is never

¹ The percentage of adsorbed TPPTS is calculated on the basis of the following formula: $\text{TPPTSads}(\%) = 100 \times \{(A_0 - A)/A_0\}$, where A_0 is the peak area of free TPPTS in water (spectrum a, Fig. 9) and A is the peak area of free TPPTS in the presence of AC-WV.

completely recovered. This demonstrates that the TPPTS ligand can be partly retained onto the carbon matrix, even under competitive conditions in the presence of the carbonate substrate.

Taken together, our experimental results are consistent with the fact that the reaction mechanism is governed by a subtle interplay of interactions involving different adsorption equilibria. Indeed, we have shown that AC-WV could adsorb the palladium/water-soluble TPPTS catalytic system and that this adsorption process was not affected to a large extent by the presence of the organic substrate. These results support the idea that the addition of carbon in the reaction medium plays a role not only in the improvement of mass-transfer of the hydrophobic reactant, but also in the regulation of the amount of water-soluble palladium complex in the pore volume. This phenomenon leads to more effective interfacial areas that promote the molecular collisions in the pore volume. Thus, we assume that the relatively apolar cavities of AC-WV act as suitable nanometer-range pockets that allow the confinement of all reactive species present in both organic and aqueous phases, as described in Scheme 3. It is worth mentioning that the system proved to be recoverable and reusable at least five times without any appreciable loss of activity, as shown recently by our group [34].

The proposed mechanism can also account for the lower relative reaction rates previously reported with the bulkiest water-soluble ligands. Indeed, this behavior seems to indicate an alteration of the mass-transfer ability of the carbon when the metal complex is stabilized by phosphanes of higher molecular

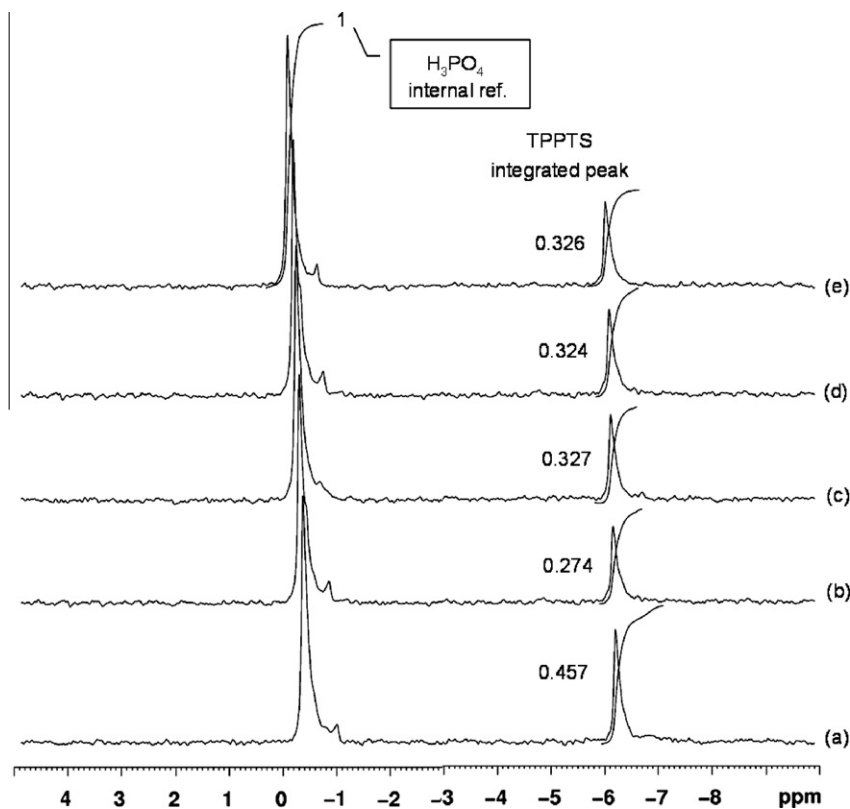
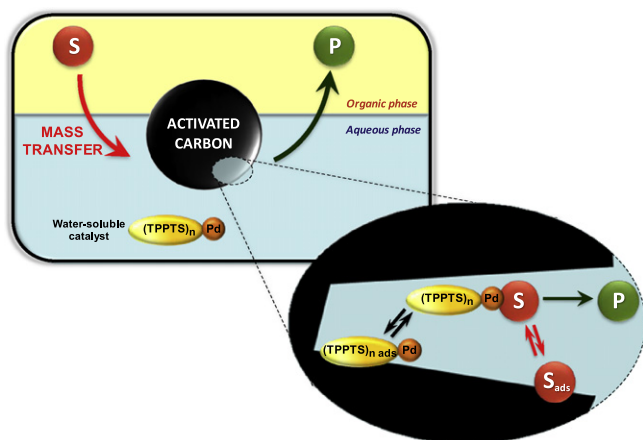


Fig. 9. Effect of addition of allylundecylcarbonate on the $^{31}\text{P}\{^1\text{H}\}$ NMR spectrum of TPPTS (10 mg) in D_2O (1 mL) at 25°C using H_3PO_4 as the external reference: (a) without AC-WV or carbonate, (b) with AC-WV and without carbonate, (c) with AC-WV and 10 μmol of carbonate, (d) with AC-WV and 30 μmol of carbonate, and (e) with AC-WV and 40 μmol of carbonate.



Scheme 3. Proposed mechanism of action of activated carbon in aqueous organometallic catalysis.

weights. This effect could result from a loss of accessible surface area for the hydrophobic allylundecylcarbonate during the catalytic course, due to a higher surface coverage by the palladium complex species or extended pore blocking by steric congestions.

5. Conclusion

In conclusion, we have described a simple and environmentally friendly strategy for enhancing the Tsuji–Trost overall reaction rates, based on the combined use of a water-soluble palladium complex and activated carbon as mass-transfer promoter. The

method allows the easy separation of the products from the catalytic suspension and catalyst recyclability without any detectable loss of activity. A number of parameters, which governs the catalytic properties of this triphasic organic–aqueous–AC system, have been identified to increase the overall reaction rate, including *adequate pore size, carbon-rich surface, hydrophobic reactants, and high water content*. It was found that the mechanism could not be ascribed to a SAPC-type mechanism. Indeed, we have established that different adsorption equilibria with the hydrophobic substrate and the organometallic complex were involved in the interactions with the carbon surface. This hypothesis was clearly supported by isothermal adsorption studies and $^{31}\text{P}\{^1\text{H}\}$ NMR experiments. Finally, it is suggested that carbons combining a high surface area, a high proportion of mesopores and a relatively apolar nature are key factors to allow the confinement and mobility of the reactants and catalyst within the porous network of the solid. These conclusions lay the foundation for future investigations to improve the performances of metal-catalyzed processes performed under biphasic conditions. In particular, experiments are currently under way to develop the use of hydrophobic mesoporous carbons with high surface areas and large pore volumes.

Acknowledgments

Dr. N. Kania is grateful to the Agence de l'Environnement et la Maitrise de l'Energie and the Région Nord-Pas de Calais for a PhD grant (2006–2009). Dr Gokulakrishnan is thankful for financial support by the Institut de Recherche en Environnement Industriel (IRENI, 2009). MeadWestvaco Corporation (Covington, USA) is gratefully acknowledged for the generous gift of the activated carbon.

Appendix A. Supplementary material

Supplementary data associated with this article can be found in the online version, at doi:10.1016/j.jcat.2010.12.005.

References

- [1] B. Cornils, W.A. Herrmann (Eds.), *Aqueous-Phase Organometallic Catalysis*, Wiley-VCH, Weinheim, 2004.
- [2] K.H. Shaughnessy, *Chem. Rev.* 109 (2009) 643.
- [3] B. Cornils, *J. Mol. Catal. A: Chem.* 143 (1999) 1.
- [4] P. Purwanto, H. Delmas, *Catal. Today* 24 (1995) 135.
- [5] H. Ding, B.E. Hanson, T. Bartik, B. Bartik, *Organometallics* 13 (1994) 3761.
- [6] M.S. Goedheijt, B.E. Hanson, J.N.H. Reek, P.C.J. Kamer, P.W.N.M. van Leeuwen, *J. Am. Chem. Soc.* 122 (2000) 1650.
- [7] M. Bortenschlager, N. Schöllhorn, A. Wittmannand, R. Weberskirch, *Chem. Eur. J.* 13 (2007) 520.
- [8] E. Paetzold, G. Oehme, *J. Mol. Catal. A: Chem.* 152 (2000) 69.
- [9] C.C. Miyagawa, J. Kupka, A. Schumpe, *J. Mol. Catal. A: Chem.* 234 (2005) 9.
- [10] H. Fu, M. Li, H. Chen, X. Li, *J. Mol. Catal. A: Chem.* 259 (2006) 156.
- [11] S.L. Desset, D.J. Cole-Hamilton, D.F. Foster, *Chem. Commun.* (2007) 1933.
- [12] C. Binkowski, J. Cabou, H. Bricout, F. Hapiot, E. Monflier, *J. Mol. Catal. A: Chem.* 215 (2004) 23.
- [13] P. Blach, D. Landy, S. Fourmentin, G. Surpateanu, H. Bricout, A. Ponchel, F. Hapiot, E. Monflier, *Adv. Synth. Catal.* 347 (2005) 1301.
- [14] F. Hapiot, L. Leclercq, N. Azaroual, S. Fourmentin, S. Tilloy, E. Monflier, *Curr. Org. Synth.* 15 (2008) 162.
- [15] F.X. Legrand, M. Sauthier, C. Flahaut, J. Hachani, C. Elfakir, S. Fourmentin, S. Tilloy, E. Monflier, *J. Mol. Catal. A: Chem.* 303 (2009) 72.
- [16] A.A. Dabbawala, J.N. Parmar, R.V. Jasra, H.C. Bajaj, E. Monflier, *Catal. Commun.* 10 (2009) 1808.
- [17] J.P. Arhancet, M.E. Davis, J.S. Merola, B.E. Hanson, *Nature* 339 (1989) 454.
- [18] J.P. Arhancet, M.E. Davis, J.S. Merola, B.E. Hanson, *J. Catal.* 121 (1990) 327.
- [19] J.P. Arhancet, M.E. Davis, B.E. Hanson, *J. Catal.* 129 (1991) 94.
- [20] J.P. Arhancet, M.E. Davis, B.E. Hanson, *J. Catal.* 129 (1991) 100.
- [21] G. Fremy, E. Monflier, J.F. Carpentier, Y. Castanet, A. Mortreux, *J. Catal.* 162 (1996) 339.
- [22] E. Fache, C. Mercier, N. Pagnier, B. Despeyroux, P. Panster, *J. Mol. Catal.* 79 (1993) 117.
- [23] K.T. Wan, M.E. Davis, *J. Catal.* 148 (1994) 1.
- [24] S. dos Santos, Y. Tong, F. Quignard, A. Choplin, D. Sinou, J.P. Dutasta, *Organometallics* 17 (1998) 78.
- [25] P. Handa, M. Stjerndahl, K. Holmberg, *Micropor. Mesopor. Mater.* 100 (2007) 146.
- [26] R.L. Kars, R.J. Best, A.A.H. Drinkenburg, *Chem. Eng. J.* 17 (1979) 201.
- [27] E. Alper, B. Wichtendahl, W.D. Deckwer, *Chem. Eng. Sci.* 35 (1980) 217.
- [28] A.A.C.M. Beenackers, W.P.M. van Swaaij, *Chem. Eng. Sci.* 48 (1993) 3109.
- [29] S. Nedeltchev, A. Schumpe, *Chem. Eng. Sci.* 60 (2005) 6504.
- [30] C. Moreno-Castilla, *Carbon* 42 (2004) 83.
- [31] L. Peereboom, B. Kenigsnecht, M. Hunter, J.E. Jackson, D.J. Miller, *Carbon* 45 (2007) 579.
- [32] F. Rodriguez-Reinoso, *Carbon* 36 (1998) 159.
- [33] C. Disser, C. Muennich, G. Luft, *Appl. Catal. A* 296 (2005) 201.
- [34] N. Kania, B. Léger, S. Fourmentin, E. Monflier, A. Ponchel, *Chem. Eur. J.* 16 (2010) 6138.
- [35] R. Gärtner, B. Cornils, H. Springer, P. Lappe, DE patent 3235030 (1982).
- [36] M. Ferreira, H. Bricout, F. Hapiot, A. Sayede, S. Tilloy, E. Monflier, *ChemSusChem* 1 (2008) 631.
- [37] H.P. Boehm, *Carbon* 32 (1994) 759.
- [38] W.A. Herrmann, J. Kellner, H. Riepl, *J. Organomet. Chem.* 389 (1990) 103.
- [39] S. Hermans, C. Diverchy, O. Demoulin, V. Dubois, E.M. Gaigneaux, M. Devillers, *J. Catal.* 243 (2006) 239.
- [40] S. Biniak, M. Pakula, G.S. Szymański, A. Swiatkowski, *Langmuir* 15 (1999) 6117.
- [41] A.A. El-Hendawy, *Carbon* 41 (2003) 713.
- [42] H. Valdés, M. Sánchez-Polo, J. Rivera-Utrilla, C.A. Zaror, *Langmuir* 18 (2002) 2111.
- [43] M. Ahmednaa, W.E. Marshall, R.M. Rao, *Bioresour. Technol.* 71 (2000) 103.
- [44] C.O. Ania, B. Cabal, C. Pevida, A. Arenillas, J.B. Parra, F. Rubiera, J.J. Pis, *Water Res.* 41 (2007) 333.
- [45] M.A. Lillo-Ródenas, D. Cazorla-Amorós, A. Linares-Solano, *Carbon* 3 (2005) 1758.
- [46] M. Beller, T.H. Riermeier, *Tetrahedron Lett.* 37 (1996) 6535.
- [47] R.L. Tseng, F.C. Wu, *J. Hazard. Mater.* 155 (2008) 277.
- [48] F. Monteil, P. Kalck, *J. Organomet. Chem.* 482 (1994) 45.
- [49] C. Amatore, E. Blart, J.P. Genêt, A. Jutand, S. Lemaire-Audoire, M. Savignac, *J. Org. Chem.* 60 (1995) 6829.
- [50] G. Papadogianakis, J.A. Peters, L. Maat, R.A. Sheldon, *J. Chem. Soc. Chem. Commun.* (1995) 1105.